

Communication

Isolation and Structural Elucidation of Unreported Prenylhydroquinone Glycoside from *Sedum kamtschaticum* Leaves and Its Effect on Hyperphosphorylated Tau Production in A β _{1–42}-Treated SH-SY5Y Cells

Seung-Eun Lee ^{1,*†}, Se Yun Jeong ^{2,†}, Yoon Seo Jang ^{2,†}, Kwang-Jin Cho ³, Jeonghoon Lee ¹, Yunji Lee ¹ and Ki Hyun Kim ^{2,*} 

¹ Department of Herbal Crop Research, National Institute of Horticultural & Herbal Science (NIHHS), Eumseong 27709, Republic of Korea; artemisia@rda.go.kr (J.L.); yoong0625@korea.kr (Y.L.)

² School of Pharmacy, Sungkyunkwan University, Suwon 16419, Republic of Korea; dlawtkark@naver.com (S.Y.J.); bbj0423@gmail.com (Y.S.J.)

³ Korean Medicine-Based Drug Repositioning Cancer Research Center, Seoul 02447, Republic of Korea; kjcho@khu.ac.kr

* Correspondence: herbin3@korea.kr (S.-E.L.); khkim83@skku.edu (K.H.K.); Tel.: +82-43-871-5755 (S.-E.L.); +82-31-290-7700 (K.H.K.)

† These authors contributed equally to this work.

Abstract: *Sedum kamtschaticum* Fischer, of the Crassulaceae family, is a perennial and medicinal plant used in Asian folk medicine to alleviate inflammatory disease and improve blood circulation. As part of our ongoing exploration into natural products, seeking to identifying bioactive compounds, we characterized, identified, and isolated an unreported bioactive compound, prenylhydroquinone glycoside (**1**), which we named kirinchoside from *S. kamtschaticum* leaves. Using high-resolution (HR)-ESIMS, NMR spectroscopic data, and enzymatic hydrolysis, followed by LC–MS analysis, we determined the structure of this isolated compound. Despite a previous report on the planar structure of compound **1** (kirinchoside), the absolute configuration of **1** had not been verified. We investigated the effects of kirinchoside on hyperphosphorylated tau (p-tau) accumulation, a hallmark of Alzheimer’s disease (AD) progression. We observed that treatment with 5 μ M kirinchoside suppressed p-tau levels by 16.9% in amyloid β (A β)_{1–42}-treated SH-SY5Y cells, compared to the negative control. These findings indicate that kirinchoside, an unreported prenylhydroquinone glycoside found in *S. kamtschaticum* leaves, could be a candidate preventive agent against AD via inhibition of p-tau accumulation.

Keywords: *Sedum kamtschaticum*; Crassulaceae; structural elucidation; prenylhydroquinone glycoside; tau; SH-SY5Y cells



Citation: Lee, S.-E.; Jeong, S.Y.; Jang, Y.S.; Cho, K.-J.; Lee, J.; Lee, Y.; Kim, K.H. Isolation and Structural Elucidation of Unreported Prenylhydroquinone Glycoside from *Sedum kamtschaticum* Leaves and Its Effect on Hyperphosphorylated Tau Production in A β _{1–42}-Treated SH-SY5Y Cells. *Separations* **2023**, *10*, 428. <https://doi.org/10.3390/separations10080428>

Academic Editor: Paraskevas D. Tzanavaras

Received: 12 June 2023

Revised: 24 July 2023

Accepted: 25 July 2023

Published: 28 July 2023



Copyright: © 2023 by the authors. Licensee MDPI, Basel, Switzerland. This article is an open access article distributed under the terms and conditions of the Creative Commons Attribution (CC BY) license (<https://creativecommons.org/licenses/by/4.0/>).

1. Introduction

Alzheimer’s disease (AD) is the primary cause of dementia, accounting for approximately 50–60% of all cases of dementia. Over the next century, the burden of AD will continue to increase, both in terms of disability and healthcare costs, with the growing number of patients predicted to reach 81 million by 2040 [1]. Intensive research on the pathogenic mechanisms of AD has shed light on the complex interaction of amyloid β aggregation and deposition, hyperphosphorylation of tau and tangle formation, neurovascular dysfunction, inflammation, mitochondrial dysfunction, cell-cycle abnormalities, and cell death induced by oxidative stress [2]. Of these pathogenic mechanisms, hyperphosphorylation of tau has been studied for its contributing role to the neuronal death underlying dementia. Tau is a protein primarily found in axons that plays a crucial role in promoting microtubule stabilization and assembly. Hyperphosphorylation of tau begins intracellularly and induces

a sequence of pathogenic events in AD, namely, the disassembly of microtubules associated with neuronal dysfunction. Hyperphosphorylated tau forms insoluble fibrils, termed neurofibrillary tangles [3]. Recent studies have demonstrated that preventing or reducing tau accumulation leads to improvements in cognitive and motor dysfunction in various animal models of AD [4]. However, currently available drugs only relieve symptoms temporarily, without providing a cure. Thus, the identification of natural bioactive products that can help prevent AD is an attractive area of study. Tau has emerged as a promising therapeutic target in the development of bioactive compounds for AD prevention.

Sedum kamtschaticum Fischer (Crassulaceae) is a perennial plant that can be commonly found in China, Japan, and Korea. The aqueous extract of *S. kamtschaticum* has been used in folk medicine to improve blood circulation and prevent inflammation [5]. Recent pharmacological studies on *S. kamtschaticum* have demonstrated that the plant extracts and their active components exhibit various therapeutic effects, including anti-carbohydrate digesting enzyme, anti-pancreatic lipase, anti-inflammatory, and antioxidant activities [6–9]. The methanol extract obtained from *S. kamtschaticum* exhibits notable inhibitory activity against mouse paw and ear edema. Additionally, it demonstrates potent analgesic activity for acetic acid-induced writhing of mouse [8]. Additionally, compared to other edible plants grown in Korea, the *S. kamtschaticum* extract contains more polyphenols and significant antioxidant activity against diphenylpicrylhydrazyl and 2,2'-azinobis-(3-ethylbenzothiazoline-6-sulfonate) radicals [9]. *S. kamtschaticum* contains many phenolic compounds such as tannins, flavonoids, coumarins, and hydroquinone [10], highlighting its potential for the discovery of bioactive compounds.

As part of our ongoing exploration into natural products, seeking to identifying bioactive compounds with potential therapeutic properties and novel structure [11–15], we investigated potential bioactive phytochemicals from *S. kamtschaticum* leaves. As a result of these investigations, a previously unreported compound (**1**; kirinchoside) was isolated from the methanol extract by high-performance liquid chromatography (HPLC) purification. The structure of the isolated compound was characterized using nuclear magnetic resonance (NMR) spectroscopy, high-resolution (HR) electrospray ionization (ESI)–mass spectroscopy (MS), and enzymatic hydrolysis combined with liquid chromatography (LC)–MS analysis. The isolated compound was tested for its effects on the production of hyperphosphorylated tau (p-tau) in amyloid β ($A\beta$)_{1–42}-treated SH-SY5Y cells.

2. Materials and Methods

2.1. General Experimental Procedures

The infrared (IR) spectra were collected utilizing a Shimadzu IRTracer-100 spectrometer (Shimadzu Scientific Korea Corp., Seoul, Republic of Korea), and the ultraviolet (UV) spectra were obtained using an Agilent 8453 UV-visible spectrophotometer (Agilent Technologies, Santa Clara, CA, USA). NMR spectra in this study were recorded on a Bruker AVANCE III 600 NMR spectrometer operating at 600 MHz for proton (¹H) NMR and 150 MHz for carbon-13 (¹³C) NMR, and the chemical shifts were reported in ppm (δ). For preparative HPLC, a K-prep LAB Series LAB300G pump equipped with a K-prep LAB Series LAB300G UV detector (YMC Triart, YMC Ltd., Kyoto, Japan) was employed. A YMC Triart-Prep C18 column (500 × 50 mm, 15 μ m; YMC Ltd.) was used, and the flow rate was set at 90 mL/min. LC–MS analysis was conducted using an Advion Compact mass electrospray ionization (ESI) spectrometer (Advion Inc., Ithaca, NY, USA) with a YMC-Triart C18 column (150 × 2.0 mm, 3 μ m) and a flow rate of 0.3 mL/min. HR-ESIMS analysis was performed with an Agilent 1290 Infinity II ultra-high-performance liquid chromatograph coupled with a G6545B Q-TOF MS system featuring a dual ESI source (Agilent Technologies). Thin-layer chromatography (TLC) was conducted using Merck-precoated silica gel F254 plates (Darmstadt, Germany) and RP-C18 F254s plates. Chromatographic spots were visualized either under UV light at wavelengths of 254 nm and 365 nm or by heating after spraying with anisaldehyde sulfuric acid.

2.2. Plant Material

In July 2018, the leaves of *S. kamtschaticum* were collected from Eumseong-gun, Chungcheongbuk-do, Korea, and subsequently dried. To ensure accurate identification, a specimen (voucher no. MPS002557) obtained from the National Institute of Horticultural and Herbal Science (NIHHS) in Eumseong, Korea, was used as a reference for comparison.

2.3. Extraction and Separation of **1**

Powdered *S. kamtschaticum* leaves (800 g) were subjected to extraction with EtOH at 85 °C. The extract was filtered twice to remove any impurities. The solvents in the extract were evaporated in vacuum at 50 °C. The crude extract (168.4 g) was stored at −20 °C until it was used. The crude EtOH extract (8.0 g) was suspended in 50% MeOH (160 mL) to a concentration of 50 mg/mL, and the dissolved extract filtered (membrane filter; 0.22 µm; Millex, Merck Millipore, Burlington, MA, USA). The LC–MS analysis of the EtOH extract obtained revealed the presence of one major peak at m/z 399.1 $[M + H]^+$. To isolate the major peak, the dissolved crude extract was isolated using preparative HPLC using a YMC Triart-Prep C18 column (500 × 50 mm, 15 µm) with a gradient system from 10% to 60% MeOH (flow rate: 90 mL/min) to furnish the compound **1** (12 mg; t_R = 22.3 min, 0.15%).

Kirinchoside (**1**)

White amorphous powder; $[\alpha]_D^{25}$ −35.5 (*c* 0.20, MeOH); UV (MeOH) λ_{max} (log ϵ) 285 (3.2) nm; IR (neat) ν_{max} 3380, 2870, 1685, 1630, 1450, 1375, 1120 cm^{-1} ; 1H (600 MHz) and ^{13}C NMR (150 MHz) (see the Table 1); (+)–ESIMS m/z 399.1 $[M + H]^+$; (+)–HR-ESIMS m/z 399.1650 $[M + H]^+$ (calculated for $C_{19}H_{27}O_9$, 399.1655).

Table 1. 1H (600 MHz) and ^{13}C NMR (150 MHz) data for compound **1** in D_2O (δ ppm).

Position	1	
	δ_H (J in Hz)	δ_C
1		127.7 s
2		129.0 s
3		149.2 s
4	6.83 d (9.0)	114.4 d
5	7.00 d (9.0)	114.8 d
6		160.9 s
7	3.65 s	34.9 t
8		180.4 s
1'	3.37 overlap	25.3 t
2'	5.10 t (6.5)	121.6 d
3'		133.7 s
4'	1.81 s	17.1 q
5'	1.71 s	24.8 q
1''	4.93 d (7.5)	102.0 d
2''	3.60 overlap	73.0 d
3''	3.60 overlap	75.5 d
4''	3.52 overlap	69.4 d
5''	3.54 overlap	76.0 d
6''	3.94 dd (12.0, 2.0); 3.77 dd (12.0, 5.5)	60.6 t

2.4. Enzymatic Hydrolysis and Absolute Configuration Determination of the Sugar Moiety of Compound **1**

To perform hydrolysis, 1.0 mg of compound **1** was treated with crude glucosidase (10 mg) sourced from almonds, and the glucosidase was purchased from Sigma-Aldrich (St. Louis, MO, USA). The hydrolysis reaction was carried out for 72 h at a temperature of 37 °C. Subsequently, the aglycone was extracted using dichloromethane (CH_2Cl_2). The absolute configuration of the sugar component present in the aqueous layer was determined using a previously established method [16].

2.5. Cell Culture

The SH-SY5Y cell line, which is derived from human neuroblastoma (SK-N-SH), was cultured in RPMI-1640 medium. The medium was supplemented with 10% horse serum, 5% fetal bovine serum, and 1% penicillin and streptomycin to support cell growth and viability [17].

2.6. Analysis of Cell Proliferation in SH-SY5Y Cells

For the measurement of SH-SY5Y cell proliferation, cells were seeded into each well of a 24-well plate (1×10^5 cells/well). The cells were then incubated for 24 h to allow for attachment and initial growth. Subsequently, the cells were then treated with 10 μ M retinoic acid (RA) for 2 days and treated with compound **1** (1.25, 2.5, 5, and 10 μ M) for 24 h. After removing the supernatant, the SH-SY5Y cells were incubated with 3-(4,5-dimethylthiazol-2-yl)-2,5-diphenyltetrazolium bromide (MTT) reagent at a concentration of 0.6 mg/mL for 1 h at 37 °C. Following the incubation, the MTT reagent was removed, and the formazan crystals formed by viable cells were dissolved in dimethyl sulfoxide. The absorbance of the resulting solution was measured at 540 nm using a microplate reader. Cell proliferation after treatment with compound **1** was calculated compared to control, which was not treated with compound **1**. The result was plotted as cell proliferation on concentration.

2.7. Analysis of p-Tau Production in SH-SY5Y Cells

For the assessment of compound **1**'s inhibitory activity on p-tau production, SH-SY5Y cells were seeded into 6-well plates (1×10^5 cells/well) and incubated for 24 h. The cells were then treated with RA (10 μ M) for 6 days and brain-derived neurotrophic factor (BDNF; 5 nM) for 2 days. Subsequently, compound **1** was applied to the cells for 2 h. Following this, 0.305 μ M amyloid β ($A\beta$)₁₋₄₂ was added to all wells except for the control well. After 48 h, the supernatant in each well was removed, and the cells were washed using ice-cold phosphate-buffered saline (PBS) and lysed. The lysates were collected and subsequently centrifuged at $13,201 \times g$ at 4 °C, for 20 min. The levels of p-tau in the supernatant were evaluated using ELISA kit, following the manufacturer's instructions (MyBioSource, Houston, TX, USA). The supernatants were added to wells of a 96-well plate and reacted with the HRP-conjugated reagent for 60 min at 37 °C. After washing four times, the wells were added with chromogen solution A and chromogen solution B and incubated for 15 min at 37 °C. After treatment with the stop solution, the optical density at 450 nm of the wells was measured. All of the assay procedures were compared to the blank and standard. Protein levels of the supernatants were also measured using the Bradford method [18]. Finally, p-tau levels (per mg protein) were calculated from the standard curve and protein content.

2.8. Statistical Analysis

The data obtained from multiple independent experiments in this study were presented as mean \pm standard deviation. To evaluate the overall significance, analysis of variance (ANOVA) was performed, followed by Duncan's multiple range test with a significance level of $p < 0.05$. The statistical analysis was conducted using version 9.4 SAS software (SAS Institute Inc., Cary, NC, USA).

3. Results and Discussion

3.1. Isolation of Compound **1**

S. kamtschaticum leaves were powdered and subsequently extracted with ethanol (EtOH) to obtain crude extracts. The crude extract underwent analysis using LC-MS, which revealed the presence of a prominent protonated molecule ion with an m/z value of 399.1 $[M + H]^+$ (Figure 1, top panel). The major peak (compound **1**) was isolated by preparative HPLC separation at a low UV wavelength (210 nm) (Figure S2). The isolated compound **1** was found to have a purity >95%, as illustrated in Figure 1.

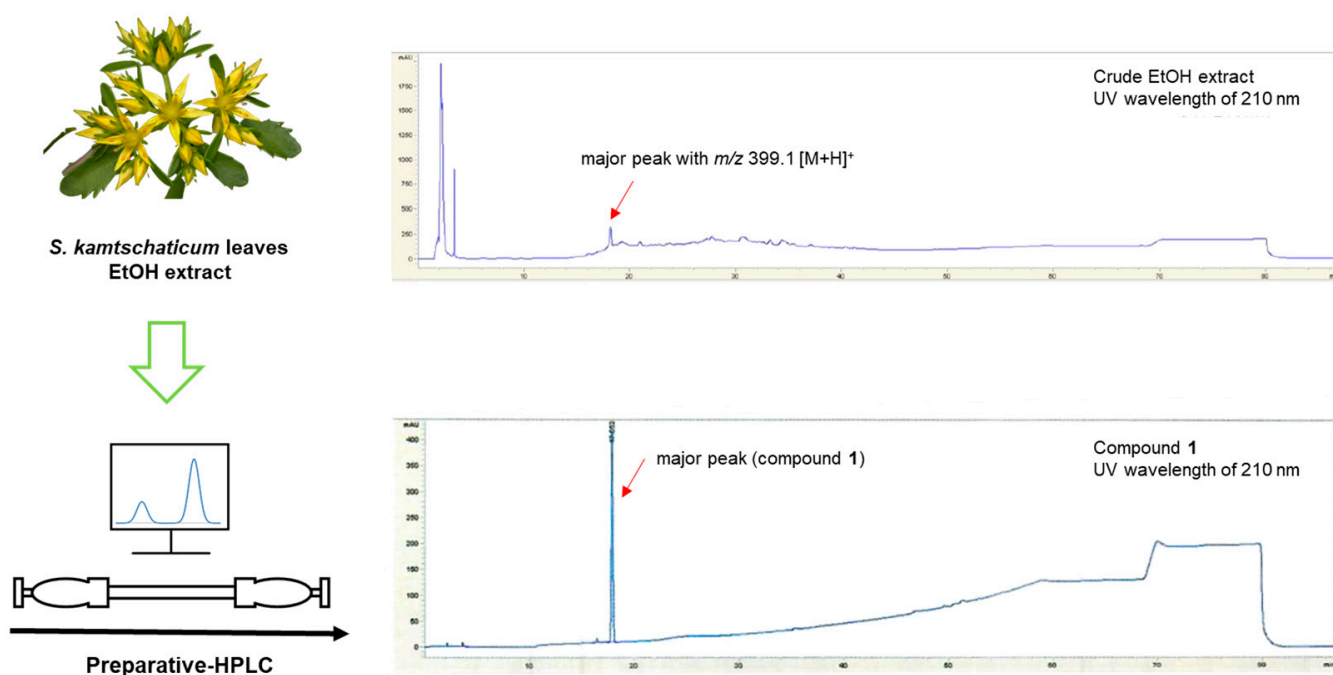


Figure 1. Separation of compound **1** from *S. kamtschaticum* leaves and HPLC–UV chromatograms of crude EtOH extract and compound **1**.

3.2. Structural Determination of Compound **1**

Compound **1** (Figure 2) was obtained as a white amorphous powder, and its molecular formula was deduced to be $C_{19}H_{26}O_9$ using HR-ESIMS. The high-resolution mass spectrometry analysis revealed a prominent $[M + H]^+$ ion peak at m/z 399.1650 (calculated for $C_{19}H_{27}O_9$, 399.1655) (Figure S1). The IR spectrum (Figure S3) of compound **1** exhibited characteristic absorptions for the functional groups of hydroxy (3380 cm^{-1}) and carbonyl (1685 cm^{-1}) moieties. The ^1H NMR data (Table 1 and Figure S4) of compound **1**, assigned using heteronuclear single quantum correlation (HSQC) experiment (Figure S7), demonstrated the existence of signals for two aromatic protons at δ_{H} 6.83 (1H, d, $J = 9.0$ Hz) and 7.00 (1H, d, $J = 9.0$ Hz), a prenyl residue composed of one olefinic proton at δ_{H} 5.10 (1H, t, $J = 6.5$ Hz), two aliphatic protons at δ_{H} 3.37 (2H, overlapped), two methyl groups at δ_{H} 1.71 (3H, s) and 1.81 (3H, s), and two additional aliphatic protons at δ_{H} 3.65 (2H, s). A β -glucopyranose residue was also identified by the anomeric proton at δ_{H} 4.93 (1H, d, $J = 7.5$ Hz) and the characteristic two double doublets at δ_{H} 3.77 (1H, dd, $J = 12.0, 5.0$ Hz) and 3.94 (1H, dd, $J = 12.0, 2.0$ Hz). As expected, the ^{13}C NMR data (Figure S5 and Figure S9) exhibited nineteen carbon resonances, showing six aromatic signals, two of which were oxygenated (δ_{C} 149.2 and 149.2), two olefinic carbons (δ_{C} 121.6 and 133.7), two methyl groups (δ_{C} 17.1 and 24.8), two methylene carbons (δ_{C} 25.3 and 34.9), and one carbonyl carbon (δ_{C} 180.4), as well as six carbons (δ_{C} 102.0, 76.0, 75.5, 73.0, 69.4, and 60.5) corresponding to a glucose moiety [16,19]. The NMR data of compound **1** displayed a signals pattern similar to reported alkylhydroquinone glycosides [20,21], and to that of 1-O- β -glucopyranosyl-1,4-dihydroxy-2-(3',3'-dimethylallyl)-benzene [22], with noticeable differences for the signals attributable to the aromatic ring, the carbonyl group (δ_{C} 180.4), and the presence of a characteristic methylene group showing singlet protons [δ_{H} 3.65 (2H, s)].

The COSY spectrum (Figure S6) analysis revealed a correlation between the methylene protons (H-1') and the olefinic proton (H-2'). Further analysis of the HMBC experiment (Figure S8) demonstrated correlations between H-4'/C-5', H-4'/C-3', H-4'/C-2', H-5'/C-4', H-5'/C-3', and H-5'/C-2'. These correlations confirmed the presence of the prenyl residue (Figure 3). It was determined that the prenyl unit was attached to C-1 by the interpretation of the HMBC correlations between H-1'/C-1 (δ_{C} 127.7), H-1'/C-2 (δ_{C} 129.0), and H-1'/C-6 (δ_{C} 160.9). The observation for HMBC correlation between an anomeric proton (H-1'') at δ_{H} 4.93 and C-6 (δ_{C} 160.9) confirmed that the glucose sugar unit was linked to C-6 (Figure 3). In

addition, the COSY spectrum indicated the key correlation between H-4 (δ_{H} 6.83) and H-5 (δ_{H} 7.00) in the aromatic ring, and the HMBC spectrum of **1** also included the correlations for H-4/C-2 (δ_{C} 129.0), H-4/C-6 (δ_{C} 160.9), H-5/C-1 (δ_{C} 127.7), and H-5/C-3 (δ_{C} 149.2). Finally, the remaining methylene proton at δ_{H} 3.65 (2H, s) displayed HMBC correlations with carbons C-1 (δ_{C} 127.7), C-2 (δ_{C} 129.0), C-3 (δ_{C} 149.2), and C-8 (δ_{C} 180.4), indicating that the acetic acid moiety was positioned to the C-2 position (Figure 3). These results helped us elucidate the gross structure of compound **1**, as depicted in Figure 2.

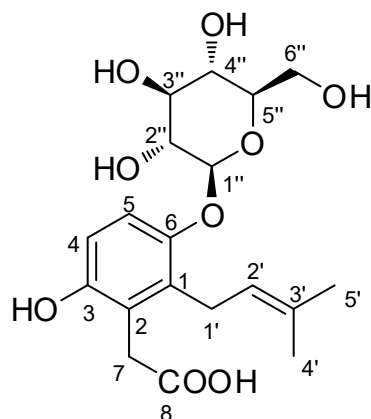


Figure 2. Chemical structure of compound **1**.

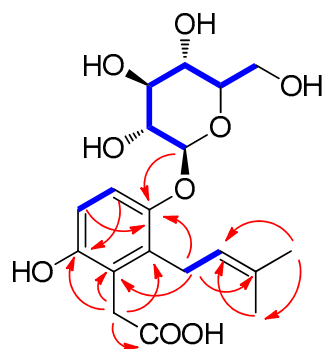


Figure 3. Key ^1H - ^1H COSY (—) and HMBC (↪) correlations for **1**.

Finally, to ascertain the absolute configuration of the sugar unit, enzymatic hydrolysis of compound **1** was conducted using glucosidase. The glucose unit's absolute configuration in compound **1** was determined to be in the D-configuration through LC-MS analysis following thiocarbamoyl-thiazolidine derivatization method (Figure S10) [23]. The 7.5 Hz coupling constant indicated the presence of the β -form of the anomeric proton in glucopyranose [24]. This observation confirmed that the sugar unit in compound **1** is β -D-glucopyranose. Consequently, the structure of **1** was successfully determined as depicted in Figure 2, and it was assigned the name as kirinchoside. A literature review revealed that the planar structure of compound **1** (kirinchoside) had been previously reported [25], but its absolute configuration had not been verified.

3.3. Evaluation of Effects of Compound **1** on p-Tau Accumulation in $\text{A}\beta_{1-42}$ -Treated SH-SY5Y Cell

To examine the impact of compound **1** on p-tau production in $\text{A}\beta_{1-42}$ -treated SH-SY5Y cells, we first evaluated cell viability following treatment with compound **1**. We observed significant increases in the proliferation rate of SH-SY5Y cells treated with different concentrations compound **1** (1.25, 2.5, 5, and 10 μM ; 129.5, 126.9, 115.5, and 119.0%, respectively) compared to that (100.0%) of the control (Figure 4A, $p < 0.05$). Next, we tested the effect of compound **1** on p-tau production. We observed that treatment with 5 μM compound **1** suppressed the production of p-tau by 16.9% in $\text{A}\beta_{1-42}$ -treated SH-SY5Y cells, compared to the

negative control (Figure 4B, $p < 0.05$), but the higher concentration (10 μM) of compound 1 did not affect the level of p-tau. Alzheimer's disease (AD) is the most common disease among age-related progressive neurodegenerative disorders [26,27]. Neuropathologic hallmarks of AD include the neurofibrillary tangles (NFTs). Mutations in the microtubule-associated protein Tau, a major component of NFTs, cause its hyperphosphorylation in AD [28]. The hyperphosphorylation of tau may contribute to the pathogenesis of AD by promoting the formation of neurofibrillary tangles from cytosolic tau, and also by inhibiting additional tau functions through disruption of its targeting to the plasma membrane [29]. These data indicate that compound 1 (kirinchoside), an unreported prenylhydroquinone glycoside, may be a candidate drug for the prevention of AD by inhibiting the accumulation of hyperphosphorylated tau.

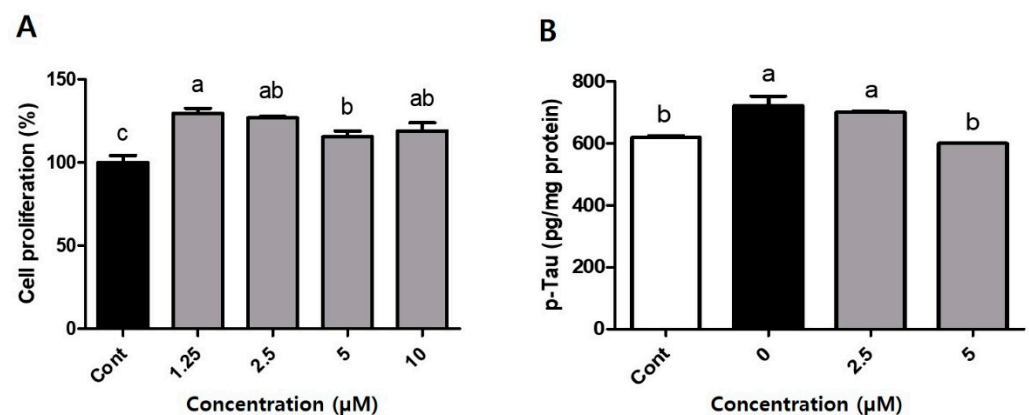


Figure 4. Effect of compound 1 on (A) cell proliferation and (B) hyperphosphorylated tau (p-tau) production in $\text{A}\beta_{1-42}$ -treated SH-SY5Y cells. (A) Cells pretreated with 10 μM retinoic acid (RA) for 2 days and then treated with compound 1 (1.25–10 μM , as indicated) for 24 h. After media removal, the MTT assay was performed and absorbances measured at 540 nm. (B) SH-SY5Y cells were treated with compound 1 (0–5 μM) for 2 h or with SF media as control. Cells were then treated with 0.305 μM $\text{A}\beta_{1-42}$ for 2 days (except control wells). p-Tau was measured using ELISA, according to the manufacturer's manual. Cont, vehicle; 0–5, compound 1 (0, 2.5, 5 μM) + $\text{A}\beta$ -treated. Statistical analysis was performed with the SAS software. a, b—significantly different from control ($p < 0.05$, Duncan's multiple range test).

Hydroquinone derivatives have been reported as potential adjuvant drugs for patients with AD because of their functions as radical scavengers, acetylcholinesterase inhibitors, and $\text{A}\beta$ -reducing activity in the brain [30–35]. Hydroquinone exhibits high nitric oxide radical scavenging activity and maximum anti-lipid peroxidation activity in vitro [30]. Hydroquinone β -D-glucoside, also known as arbutin, improves spatial memory and reduces oxidative and nitrosative stress in the serum and hippocampus [32]. Berberine-hydroquinone hybrid molecules display better antioxidant activity and inhibit $\text{A}\beta$ aggregation and cholinesterase in vitro, compared to berberine alone [33]. Derivatives of avarol, a marine sesquiterpenoid hydroquinone, exhibit non-hepatotoxic neuroprotective activity and acetylcholine esterase inhibition [34]. Moreover, a mouse model of AD exposed to a diet containing tert-butylhydroquinone displayed dramatically reduced brain $\text{A}\beta$ and enhanced levels of glutathione, an important antioxidant [35]. However, the inhibitory effects of hydroquinone derivatives on phosphorylated tau accumulation had not been investigated.

The accumulation of phosphorylated tau protein has been identified as a crucial factor in the development and progression of AD [4]. As a result, targeting tau has become an important focus in the search for effective therapeutic strategies for AD prevention [4]. Inhibiting the accumulation of phosphorylated tau holds great significance in this regard. By developing bioactive compounds that can effectively inhibit the phosphorylation of tau, researchers have attempted to prevent the abnormal aggregation and formation of neurofibrillary tangles, which are characteristic pathological hallmarks of AD. These neurofibrillary

tangles contribute to neuronal dysfunction, synaptic loss, and ultimately cognitive decline [3,4]. Inhibitory effects on phosphorylated tau accumulation are also important because they can potentially disrupt the cascade of events that lead to neurodegeneration in AD. By preventing or reducing the accumulation of phosphorylated tau, these bioactive compounds have the potential to alleviate cognitive impairment and neurological deficits associated with AD. Furthermore, inhibiting phosphorylated tau accumulation may help preserve neuronal integrity and function, as well as maintain synaptic connectivity [3,4]. This could potentially slow down or halt the progression of AD and improve the overall quality of life for affected individuals. Thus, the development of bioactive compounds with inhibitory effects on phosphorylated tau accumulation represents a promising avenue for AD prevention and treatment. By targeting tau pathology, these compounds have the potential to address one of the key pathological features of the disease and may contribute to the development of effective therapeutic interventions for AD.

4. Conclusions

An unreported prenylhydroquinone glycoside (kirinchoside) was isolated from *S. kamtschaticum* leaves, and its structure was fully elucidated via data interpretation from 1D and 2D NMR spectra, HR-ESIMS analysis, and enzymatic hydrolysis combined with LC/MS analysis [36,37]. The planar structure of compound **1** (kirinchoside) has been previously reported [25]; however, the reported NMR assignment did not match that of compound **1**, indicating that the isolated compound **1** was different from the one previously reported. We found that treatment with kirinchoside resulted in a partial inhibition of the p-tau production in A β _{1–42}-treated SH-SY5Y cells. These findings suggest appropriate experimental data that support the hypothesis that kirinchoside is a candidate preventive agent against AD.

Supplementary Materials: The following are available online at <https://www.mdpi.com/article/10.3390/separations10080428/s1>: Figure S1: HR-ESIMS data of **1**, Figure S2: UV spectrum of **1**, Figure S3: IR spectrum of **1**, Figure S4: ¹H NMR spectrum of **1** (D₂O, 600 MHz), Figure S5: ¹³C NMR spectrum of **1** (D₂O, 150 MHz), Figure S6: The ¹H-¹H COSY spectrum of **1**, Figure S7: HSQC spectrum of **1**, Figure S8: HMBC spectrum of **1**, Figure S9: DEPT135 spectrum of **1**, and Figure S10: LC/MS analysis for absolute configuration determination of the sugar moiety of compound **1**.

Author Contributions: Conceptualization, S.-E.L. and K.H.K.; formal analysis, K.-J.C. and Y.S.J.; resources, J.L. and Y.L.; investigation, S.-E.L. and K.H.K.; writing—original draft preparation, S.Y.J. and S.-E.L.; writing—review and editing, S.-E.L. and K.H.K.; visualization, S.Y.J. and Y.S.J.; supervision, S.-E.L.; project administration, S.-E.L.; funding acquisition, S.-E.L. All authors have read and agreed to the published version of the manuscript.

Funding: This study was supported by the Research R&D Project (PJ01508901) of the RDA, Republic of Korea.

Institutional Review Board Statement: Not applicable.

Informed Consent Statement: Not applicable.

Data Availability Statement: The data presented in this study are available on request from the corresponding author.

Conflicts of Interest: The authors declare no conflict of interest.

References

1. Ferri, C.P.; Prince, M.; Brayne, C.; Brodaty, H.; Fratiglioni, L.; Ganguli, M.; Hall, K.; Hasegawa, K.; Hendrie, H.; Huang, Y.; et al. Global prevalence of dementia: A Delphi consensus study. *Lancet* **2005**, *366*, 2112–2117. [[CrossRef](#)]
2. Blennow, K.; de Leon, M.J.; Zetterberg, H. Alzheimer's disease. *Lancet* **2006**, *368*, 387–403. [[CrossRef](#)] [[PubMed](#)]
3. Iqbal, K.; Alonso Adel, C.; Chen, S.; Chohan, M.O.; El-Akkad, E.; Gong, C.X.; Khatoon, S.; Li, B.; Liu, F.; Rahman, A.; et al. Tau pathology in Alzheimer disease and other tauopathies. *Biochim. Biophys. Acta* **2005**, *1739*, 198–210. [[CrossRef](#)] [[PubMed](#)]
4. Jadhav, S.; Avila, J.; Scholl, M.; Kovacs, G.G.; Kovari, E.; Skrabana, R.; Evans, L.D.; Kontsekova, E.; Malawska, B.; de Silva, R.; et al. A walk through tau therapeutic strategies. *Acta Neuropathol. Commun.* **2019**, *7*, 22. [[CrossRef](#)]

5. Bae, K. *The Medicinal Plants of Korea*; Kyohaksa Publishing Co., Ltd.: Seoul, Republic of Korea, 2000; Volume 260.
6. Kim, S.-H.; Kwon, C.-S.; Lee, J.-S.; Son, K.-H.; Lim, J.-K.; Kim, J.-S. Inhibition of carbohydrate-digesting enzymes and amelioration of glucose tolerance by Korean medicinal herbs. *Prev. Nutr. Food Sci.* **2002**, *7*, 62–66. [[CrossRef](#)]
7. Lee, Y.M.; Kim, Y.S.; Lee, Y.; Kim, J.; Sun, H.; Kim, J.H.; Kim, J.S. Inhibitory activities of pancreatic lipase and phosphodiesterase from Korean medicinal plant extracts. *Phytother. Res.* **2012**, *26*, 778–782. [[CrossRef](#)]
8. Kim, D.W.; Son, K.H.; Chang, H.W.; Bae, K.; Kang, S.S.; Kim, H.P. Anti-inflammatory activity of *Sedum kamtschaticum*. *J. Ethnopharmacol.* **2004**, *90*, 409–414. [[CrossRef](#)]
9. Lee, Y.-M.; Bae, J.-H.; Jung, H.-Y.; Kim, J.-H.; Park, D.-S. Antioxidant activity in water and methanol extracts from Korean edible wild plants. *J. Korean Soc. Food Sci. Nutr.* **2011**, *40*, 29–36. [[CrossRef](#)]
10. Korul'kin, D.Y. Chemical composition of certain *Sedum* species of Kazakhstan. *Chem. Nat. Compd.* **2001**, *37*, 219–223. [[CrossRef](#)]
11. Lee, B.S.; So, H.M.; Kim, S.; Kim, J.K.; Kim, J.C.; Kang, D.M.; Ahn, M.J.; Ko, Y.J.; Kim, K.H. Comparative evaluation of bioactive phytochemicals in *Spinacia oleracea* cultivated under greenhouse and open field conditions. *Arch. Pharm. Res.* **2022**, *45*, 795–805. [[CrossRef](#)]
12. Cho, H.; Kim, K.H.; Han, S.H.; Kim, H.-J.; Cho, I.-H.; Lee, S. Structure determination of heishuixiecaoline A from *Valeriana fauriei* and its content from different cultivated regions by HPLC/PDA Analysis. *Nat. Prod. Sci.* **2022**, *28*, 181–186. [[CrossRef](#)]
13. Yu, J.S.; Jeong, S.Y.; Li, C.S.; Oh, T.; Kwon, M.; Ahn, J.S.; Ko, S.K.; Ko, Y.J.; Cao, S.G.; Kim, K.H. New phenalenone derivatives from the Hawaiian volcanic soil-associated fungus *Penicillium herquei* FT729 and their inhibitory effects on indoleamine 2,3-dioxygenase 1 (IDO1). *Arch. Pharm. Res.* **2022**, *45*, 105–113. [[CrossRef](#)] [[PubMed](#)]
14. Lee, S.R.; Lee, B.S.; Yu, J.S.; Kang, H.; Yoo, M.J.; Yi, S.A.; Han, J.W.; Kim, S.; Kim, J.K.; Kim, J.C.; et al. Identification of anti-adipogenic withanolides from the roots of Indian ginseng (*Withania somnifera*). *J. Ginseng Res.* **2022**, *46*, 357–366. [[CrossRef](#)] [[PubMed](#)]
15. Lee, K.H.; Kim, J.K.; Yu, J.S.; Jeong, S.Y.; Choi, J.H.; Kim, J.C.; Ko, Y.J.; Kim, S.H.; Kim, K.H. Ginkwanghols A and B, osteogenic coumaric acid-aliphatic alcohol hybrids from the leaves of *Ginkgo biloba*. *Arch. Pharm. Res.* **2021**, *44*, 514–524. [[CrossRef](#)]
16. Ha, J.W.; Yu, J.S.; Lee, B.S.; Kang, D.-M.; Ahn, M.-J.; Kim, J.K.; Kim, K.H. Structural characterization of withanolide glycosides from the roots of *Withania somnifera* and their potential biological activities. *Plants* **2022**, *11*, 767. [[CrossRef](#)]
17. Lee, S.; Jang, G.; Jung, J.; Park, S.; Lee, J.; Lee, Y.; Lee, J.; Ji, Y.; Choi, J.; Kim, G. Memory-Improving activity of the flower extract from *Chrysanthemum boreale* (Makino) Maskino in scopolamine-treated rodents. *Processes* **2023**, *11*, 159. [[CrossRef](#)]
18. Akhter, H.; Katre, A.; Li, L.; Liu, X.; Liu, R.M. Therapeutic potential and anti-amyloidosis mechanisms of tert-butylhydroquinone for Alzheimer's disease. *J. Alzheimer's Dis.* **2011**, *26*, 767–778. [[CrossRef](#)]
19. Alishir, A.; Yu, J.S.; Park, M.; Kim, J.C.; Pang, C.; Kim, J.K.; Jang, T.S.; Jung, W.H.; Kim, K.H. Ulmusakidian, a new coumarin glycoside and antifungal phenolic compounds from the root bark of *Ulmus davidiana* var *japonica*. *Bioorg. Med. Chem. Lett.* **2021**, *36*, 127828. [[CrossRef](#)]
20. David, J.M.; Chávez, J.P.; Chai, H.-B.; Pezzuto, J.M.; Cordell, G.A. Two new cytotoxic compounds from *Tapirira guianensis*. *J. Nat. Prod.* **1998**, *61*, 287–289. [[CrossRef](#)]
21. Cherchar, H.; Lehbili, M.; Berrehal, D.; Morjani, H.; Alabdul Magid, A.; Voutquenne-Nazabadioko, L.; Kabouche, A.; Kabouche, Z. A new 2-alkylhydroquinone glucoside from *Phagnalon saxatile* (L.) Cass. *Nat. Prod. Res.* **2018**, *32*, 1010–1016. [[CrossRef](#)]
22. Gongora, L.; Giner, R.M.; Manez, S.; del Carmen Recio, M.; Rios, J.L. New prenylhydroquinone glycosides from *Phagnalon rupestre*. *J. Nat. Prod.* **2001**, *64*, 1111–1113. [[CrossRef](#)] [[PubMed](#)]
23. Alishir, A.; Kim, K.H. Antioxidant phenylpropanoid glycosides from *Ginkgo biloba* fruit and identification of a new phenylpropanoid glycoside, ginkgopanoside. *Plants* **2021**, *10*, 2702. [[CrossRef](#)]
24. Coxon, B. Two-dimensional J-resolved proton nuclear magnetic resonance spectrometry of hydroxyl-coupled. α - and β -D-glucose. *Anal. Chem.* **1983**, *55*, 2361–2366.
25. Ren, F.X.; Zhao, Y.M.; Zhang, A.J.; Yang, Y.; Zhang, Y. Extraction Method of Effective Components from Chinese Medicine Pyrola and Its Application for Treating Hemorrhage and/or Pain-Related Disease. China CN102204937A, 5 October 2011.
26. Kwan, K.K.L.; Yun, H.; Dong, T.T.X.; Tsim, K.W.K. Ginsenosides attenuate bioenergetics and morphology of mitochondria in cultured PC12 cells under the insult of amyloid beta-peptide. *J. Ginseng Res.* **2021**, *45*, 473–481. [[CrossRef](#)]
27. Zhang, H.; Su, Y.; Sun, Z.; Chen, M.; Han, Y.; Li, Y.; Dong, X.; Ding, S.; Fang, Z.; Li, W.; et al. Ginsenoside Rg1 alleviates A β deposition by inhibiting NADPH oxidase 2 activation in APP/PS1 mice. *J. Ginseng Res.* **2021**, *45*, 665–675. [[CrossRef](#)]
28. Giovinazzo, D.; Bursac, B.; Sbodio, J.I.; Nalluru, S.; Vignane, T.; Snowman, A.M.; Albaracarys, L.M.; Sedlak, T.W.; Torregrossa, R.; Matthew Whiteman, M.; et al. Hydrogen sulfide is neuroprotective in Alzheimer's disease by sulfhydrating GSK3 β and inhibiting Tau hyperphosphorylation. *Proc. Natl. Acad. Sci. USA* **2021**, *118*, e2017225118. [[CrossRef](#)]
29. Pooler, A.M.; Hanger, D.P. Functional implications of the association of tau with the plasma membrane. *Biochem. Soc. Trans.* **2010**, *38*, 1012–1015. [[CrossRef](#)]
30. Jamwal, V.S.; Mishra, S.; Singh, A.; Kumar, R. Free radical scavenging and radioprotective activities of hydroquinone in vitro. *J. Radioprot. Res.* **2014**, *2*, 37–45.
31. Conforti, F.; Rigano, D.; Formisano, C.; Bruno, M.; Loizzo, M.R.; Menichini, F.; Senatore, F. Metabolite profile and in vitro activities of *Phagnalon saxatile* (L.) Cass. relevant to treatment of Alzheimer's disease. *J. Enzyme Inhib. Med. Chem.* **2010**, *25*, 97–104. [[CrossRef](#)]
32. Dastan, Z.; Pouramir, M.; Ghasemi-Kasman, M.; Ghasemzadeh, Z.; Dadgar, M.; Gol, M.; Ashrafpour, M.; Pourghasem, M.; Moghadamnia, A.A.; Khafri, S. Arbutin reduces cognitive deficit and oxidative stress in animal model of Alzheimer's disease. *Int. J. Neurosci.* **2019**, *129*, 1145–1153. [[CrossRef](#)]

33. Jiang, H.; Wang, X.; Huang, L.; Luo, Z.; Su, T.; Ding, K.; Li, X. Benzenediol-berberine hybrids: Multifunctional agents for Alzheimer's disease. *Bioorg. Med. Chem.* **2011**, *19*, 7228–7235. [[CrossRef](#)]
34. Tommonaro, G.; García-Font, N.; Vitale, R.M.; Pejin, B.; Iodice, C.; Canadas, S.; Marco-Contelles, J.; Oset-Gasque, M.J. Avarol derivatives as competitive AChE inhibitors, non hepatotoxic and neuroprotective agents for Alzheimer's disease. *Eur. J. Med. Chem.* **2016**, *122*, 326–338. [[CrossRef](#)]
35. Bradford, M.M.A. Rapid and sensitive method for the quantitation of microgram quantities of protein utilizing the principle of protein-dye binding. *Anal. Biochem.* **1976**, *72*, 248–254. [[CrossRef](#)]
36. Han, K.M.; Hwang, J.; Lee, S.H.; Park, B.; Kim, H.; Baek, S.Y. Quantitative Analysis and Enantiomeric Separation of Ephedra Alkaloids in Ma Huang Related Products by HPLC-DAD and UPLC-MS/MS. *Nat. Prod. Sci.* **2022**, *28*, 168–180. [[CrossRef](#)]
37. Kang, K.B.; Lee, D.Y.; Sung, S.H. LC-MS/MS-Based Comparative Investigation on Chemical Constituents of Six Aster Species Occurring in Korea. *Nat. Prod. Sci.* **2021**, *27*, 257–263. [[CrossRef](#)]

Disclaimer/Publisher's Note: The statements, opinions and data contained in all publications are solely those of the individual author(s) and contributor(s) and not of MDPI and/or the editor(s). MDPI and/or the editor(s) disclaim responsibility for any injury to people or property resulting from any ideas, methods, instructions or products referred to in the content.